

Static Analysis of Selected Design Solutions for Weight-Reduced Gears

Tomasz Dziubek¹, Bartłomiej Sobolewski¹, Grzegorz Budzik¹, Małgorzata Gontarz^{1*}

¹ Rzeszow University of Technology, Faculty of Mechanical Engineering and Aeronautics, Department of Mechanical Engineering, Powstańców Warszawy 12 Av., Rzeszów 35-959, Poland

* Corresponding author's e-mail: m.gontarz@prz.edu.pl

ABSTRACT

The paper presents an analysis of selected design solutions for spur gears with reduced weight, in which the results obtained are compared to a solid gear without modifications. The reduction of the weight of the gears is of particular importance, among others in the automotive and aviation industries, where it reduces energy consumption, and thus CO₂ emissions. It is also important to remember to maintain the required strength parameters when reducing the mass of the gear. This article focuses on the analysis of deformation and stress due to a given load on the considered weight-reduced gears. The values of the obtained static analysis results of the reduced-weight gears were also compared to the base gear.

Keywords: gear, mass reduction, static analysis, selected design solutions, modification.

INTRODUCTION

Gears are the most important element in the field of mechanical engineering especially for industry, automotive, and aviation, mainly in power transmission where variable load and speed are required to operate machines [1–5]. Straight gears, or cylindrical gears, are the most common type of gear because of the simplicity of design and manufacture, and because they are cost-effective and require less maintenance [2, 6–8]. They are usually used to transfer power to parallel shafts [9–11]. Many analyses are presently being conducted to determine when damage or defects occur due to gear bending. From these, it can be concluded that bending failures usually occur when the yield strength of the material is exceeded [3, 6, 9, 12]. With the increase in interest, as well as the frequency of use of gears, designing a gearbox for the required conditions has become a demanding task [13–14]. Today, automotive components, particularly rotating parts in the powertrain— including gears— are designed to be as light as possible, to reduce fuel consumption and thus CO₂ emissions,

among other things [15–16]. First of all, reducing the weight of the gear transmission is important in household appliances, where the gears are obtained by injection methods from polymer materials, in which reducing their weight is important for saving material while maintaining durability and wear resistance while ensuring proper cooperation, where the disc affects the meshing conditions. Of particular importance in the automotive and aviation industries is the reduction of the weight of the gear transmission, which improves the ratio of the weight of the transmission to the transmitted power and reduce the negative impact of the dynamic phenomena occurring during its operation [1, 4]. Increasing the efficiency of the gearbox by obtaining lower friction loss, lower emissions, and lower lubrication consumption is an area of intense research [17]. By using lightweight gear materials (e.g. polymers), optimizing lubrication consumption, and modifying the gear (e.g. optimizing tooth thickness [18]), higher efficiency can be achieved in gearboxes [19–21]. It is also possible to observe an improvement in the properties of modern materials in the area,

e.g. plastic deformation and the application of additional coatings [22]. Taking into account the above considerations and the conducted literature analysis, the paper undertakes an investigation of the effect of changing the design of the gear disc between the hub and the toothed rim, to reduce the weight of the design in relation to the solid gear. On the basis of the conducted review, it was found that the most frequently used variants of gears with a reduced mass are gears with recesses, which allow obtaining a gear with a disk placed symmetrically in relation to the toothed rim. Relief holes are also used. Typical solutions of gears with a reduced mass are shown in Figure 1. The presented analysis aims to present the typical solutions of gears with reduced mass, used in machine building (such as *MB2*, *MB3*, *MB6* and *MB7*) and non-typical (such as *MB4* and *MB5*), that are possible to produce using incremental technologies with decremental methods. The article focuses on the analysis of the stresses occurring in the disc. This investigation provides the basis for another static analysis of gears manufactured from polymeric materials using additive manufacturing (AM) technology. The rationale for the analysis is the growing interest in polymers and AM in the industry. Additive printing allows you to generate complex shapes that are impossible to achieve with conventional methods. Polymer materials are used for gears (including low-, medium-, and even high-power transmission in automotive engineering in particular) because of their lighter weight, better noise dampening capability, and low manufacturing costs compared to metal gears [23–24]. Increasingly, additional fillers are added to basic polymer materials, due to fact that composite materials generally show better properties (e.g. improved hardness and tensile strength) than homogeneous and pure materials [25–26]. When constructing weight-reduced gears, symmetrical gears were selected for analysis as it was concluded, based on a review of publications, that such an arrangement of the disc would result in reduced deformation due to its design (its location relative to the rim and hub of the gear) [1, 27–28].

DEVELOPMENT OF RESEARCH MODELS OF SELECTED DESIGN SOLUTIONS

A spur gear with a modulus of 2.5 mm, a number of teeth equal to 35, an outline angle α equal to 20° , and a pitch diameter of 87.5 mm was



Fig. 1. Examples of gears with reduced weight

selected for the analysis. The width of the gear rim was 27.5 mm. Figure 2 is an illustrative diagram showing the structure of the gear. Only the disc was modified- the hub and the toothed rim are elements that are constant in each of the gears analysed.

Preliminary topology optimization of the solid gear was carried out in the Autodesk environment, assuming a weight reduction of 30%. After the simplified analysis was performed, an example solution of the gear with reduced mass was obtained, which is presented in Figure 3B. During the analysis, it was noticed that it was

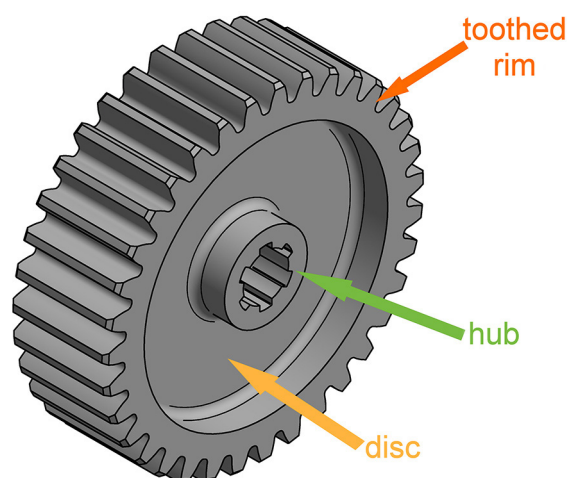


Fig. 2. Diagram showing the gear structure on the example of the *MB2* gear

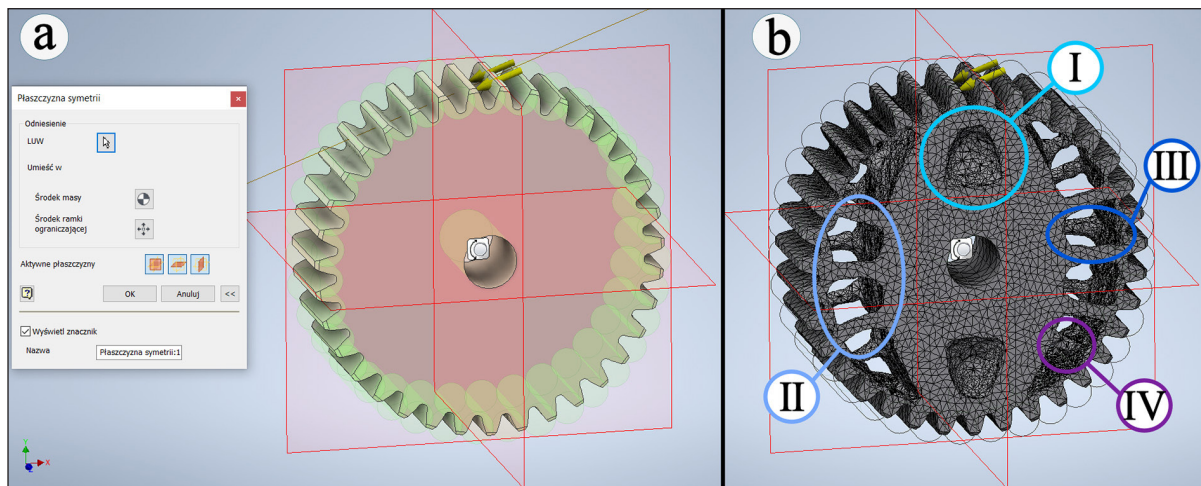


Fig. 3. Settings of the symmetry plane in topology optimization in Autodesk software (a) and solution of preliminary topological optimization of a solid gear MB1 with marked separated structures: I - disc, II - openwork structure, III - shell structure, IV - ribs (b)

not possible to set the symmetry relative to the axis of the optimized gear due to the limitations of the applied system, as presented in Figure 3A, therefore the obtained solution cannot be directly implemented to create gear with a reduced mass, because in the case of a disc, it is important to keep the geometry that is symmetrical relative to the axis. As can be seen from the presented solution, the program applied a solution in which the disc mass was reduced (Fig. 3B–I), an openwork construction (Fig. 3B–II), and a shell construction (Fig. 3B–III) were used. It can also be noticed that in the solution proposed by the software there are ribs (Fig. 3B–IV), which reinforce the structure of the gear with a reduced mass.

Based on the performed preliminary topological optimization and literature review, four design options for weight-reduced gears were selected and produced (Table 1). The models were designed and built in the Autodesk Inventor Professional 2021 environment [1, 29–30].

The gear including the rim was created in Inventor 2021 using the generator [29–30]. In the following steps, the hub and disc were created using solid modelling related commands and modified to reduce their weight. It was decided to create a cylindrical opening instead of a spline in the hub as, during the preliminary analyses of selected design solutions for gears with reduced weight, singularities occurred in the place of creating the spline, the so-called numerical notches which did not disappear despite the mesh compaction, and which disturbed the results of the conducted analyses.

Table 1 shows selected weight-reduced gears with the designations used.

Type *MB1* (Table 1) is a solid gear, without transformations, which forms the basis for design modifications of the weight-reduced gear disc. Therefore, this gear provides a reference for comparing the effects of weight reduction, which is presented later in the article.

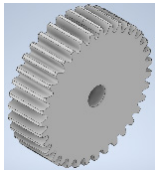
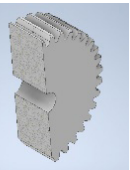

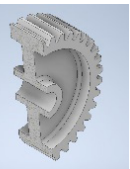

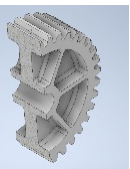
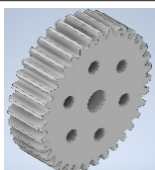
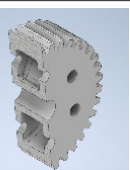
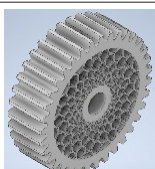
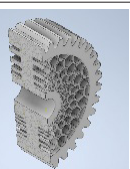

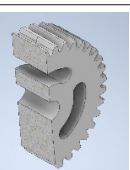


Type *MB2* (Table 1) is a symmetrical recess gear with a 10 mm thick disc. The sharp edges between the disc and the rim and hub have been rounded off to a radius of 2 mm.

The *MB3* gear (Table 1) represents a symmetrical gear with a 10 mm thick disc with six ribs arranged concentrically in relation to the gear's axis of rotation. The thickness of the rib is 3 mm. The sharp edges between the disc, rim, and hub structural components have been eliminated with a 2 mm rounding.

The *MB4* gear (Table 1) is a hollow shell gear with symmetrical discs located outside the gear rim (distance between discs: 17.5 mm; thickness of each disc: 5 mm) with six ribs, each 3 mm thick, with inspection openings in the form of $\varnothing 10$ mm diameter cylindrical holes placed on a $\varnothing 50$ mm diameter circle. The sharp edges inside the shell structure of this gear are also eliminated by rounding 2 mm.

The *MB5* gear (Table 1) presents a symmetrical gear wheel with a 10 mm thick disc, the structure of which resembles a “honeycomb” arranged concentrically with respect to the gear's axis of rotation. The thickness of the walls present in the

Table 1. Types and designations of used weight-reduced gears

No.	Description	Mark	View (CAD model)	
1	Solid gear (Base)	MB1		
2	Symmetrical gear with a 10 mm thick disc	MB2		
3	Symmetrical gear with a 10 mm thick disc with ribs	MB3		
4	Hollow shell gear with ribs and inspection holes	MB4		
5	Honeycomb gear with a 10 mm thick disc	MB5		
6	Gear with bean-shaped holes	MB6		
7	Symmetrical gear with a 10 mm thick disc with ribs with holes	MB7		

disc was set to 1 mm, in which the sharp edges were rounded with a radius equal to 0.5 mm.

The *MB6* gear (Table 1) presents a symmetrical gear with three bean-shaped holes. The radius of the “bean” is 5 mm and the angle between the center of the rounds-off the bean is 70°. These holes were arranged on a $\varnothing 50$ mm diameter circle.

The *MB7* gear (Table 1) is created on the basis of the *MB3* gear, but additionally has $\varnothing 10$ mm diameter cylindrical holes placed on a $\varnothing 50$ mm diameter circle.

PERFORMANCE OF STATIC ANALYSIS USING MES

Static analysis in the Autodesk Inventor Nastran 2021 environment was performed on the test models shown in Table 1 by loading the tooth with the resultant force due to the meshing as a result of loading the gear with a moment equal to 50 Nm. In the analysis performed, the gear was locked while the calculated resultant force was applied to one tooth. Figure 4–A shows the method of applying the gear force to the side of a tooth. The force was applied to an ellipse-shaped fragment of the tooth side. Figure 4–B shows the gear locking by applying a pin mate at the mid-point of the gear axis of rotation. The same initial conditions were assumed for each gear option. For each gear analysed, a steel material was determined and selected from the list of materials found in the Nastran 2021 environment. The grid size of the gear was set to 1 mm (Fig. 5–A), while the grid was compacted to 0.5 mm at and near the point where the force was applied (Fig. 5–B). Figure 6 shows the applied convergence settings – the maximum number of refinements was set to 10, and the stop criteria to 2%.

The static analysis was designed to determine the effect of the weight-reducing gear design modifications analysed on strength properties. After the analysis, several parameters were taken into consideration such as: displacement (max) [mm], displacement along the Z-axis (max) [mm], von Mises stress (max) [MPa], volume [mm³], and principal moment of inertia I3 [kg/mm²]. Table 2 shows the obtained results for the considered solutions along with a percentage comparison of the obtained parameter values with respect to the solid gear (*MB1*).

Based on the results presented in Table 2, graphs were prepared and are shown in Figures 7–12.

Comparing the displacement (max) values obtained, it was found that the *MB3* (ribbed disc) and *MB5* (honeycomb) gears suffered the least deformation compared to the *MB1* solid gear (Fig. 7). Considering the displacement along the Z-axis (max), the most advantageous option of the weight-reduced gear are the *MB3* ribbed disc gear (Fig. 8) and *MB7* ribbed disc gear with holes (Fig. 8), since among the analysed gears it achieved the lowest value of the analysed parameter. The gear with the *MB2* disc obtained the highest values of von Mises stress (max) (Fig. 9)

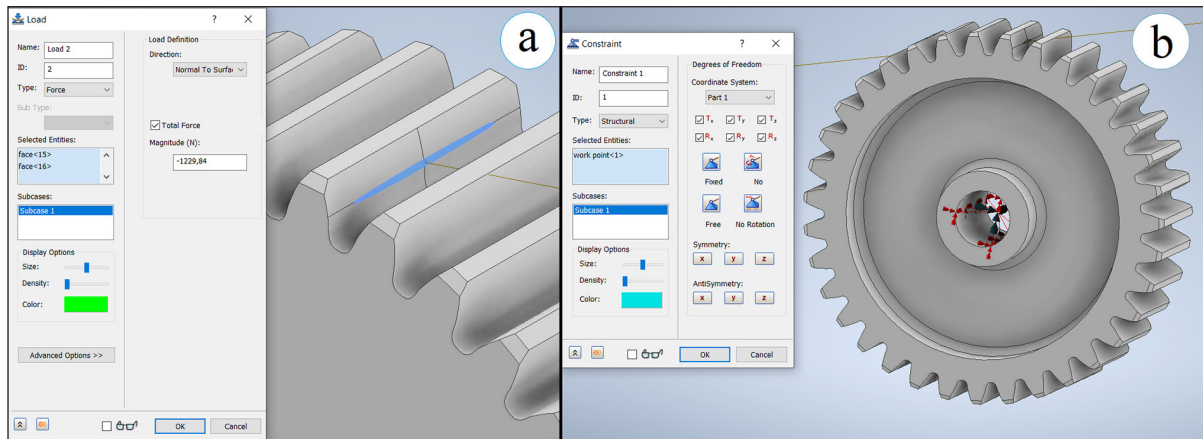


Fig. 4. Presentation of the method of applying force (a) and immobilizing the analysing gear (b) on the example of the MB2 gear

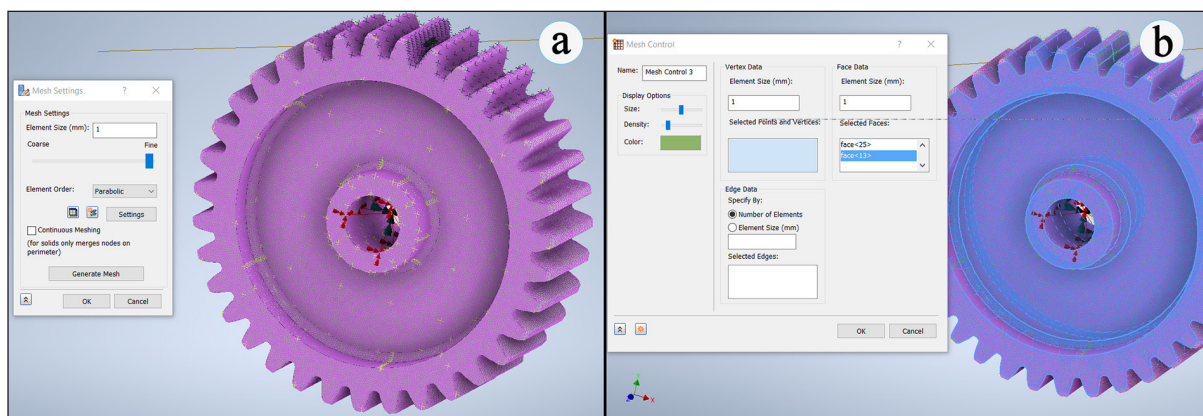


Fig. 5. Global settings of the model mesh (a) and local settings of the mesh in places close to the applied force (b) on the example of the MB2 gear

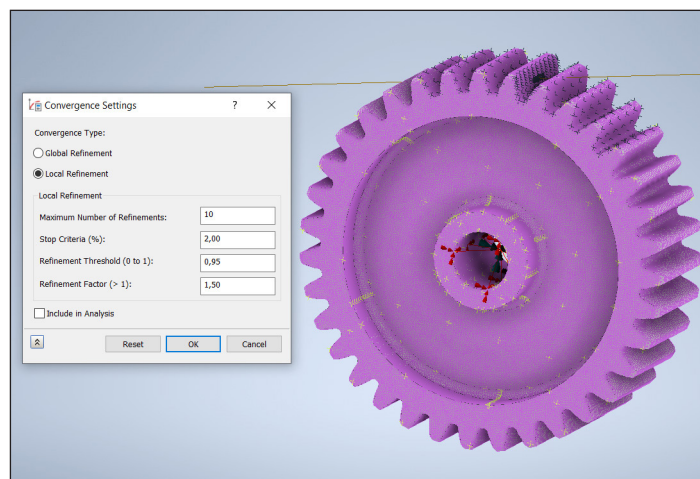


Fig. 6. Convergence settings of the static analysis on the example of MB2 gear

and underwent the greatest volume reduction (Fig. 10) relative to the gear designs analysed. The values of the principal moment of inertia I_3 of the MB2 (disc), MB3 (ribbed disc), MB4 (shell), and MB7 (ribbed disc gear with holes)

gears are comparable (within 900–950 kg/mm²) and relative to the MB1 base gear, they experienced the greatest decrease (Fig. 11).

Analysing the graph shown in Figure 12, the values of displacement (max) [mm] for the MB2

Table 2. Summary of the static analysis results for the selected weight-reduced gears

Parameter \ Mark	MB1	MB2	MB3	MB4	MB5	MB6	MB7
<i>P</i> [mm]	0.0050	0.0068	0.0063	0.0068	0.0060	0.0069	0.0066
<i>P</i> value relative to <i>MB1</i> [(<i>PA</i> − <i>PB</i>)/ <i>PB</i> ×100%] [%]	–	↑ 34.77	↑ 24.21	↑ 35.58	↑ 19.53	↑ 36.34	↑ 30.44
<i>PZ</i> [mm]	0.00038	0.00037	0.00035	0.00040	0.00037	0.00038	0.00035
<i>PZ</i> value relative to <i>MB1</i> [(<i>PZA</i> − <i>PZB</i>)/ <i>PZB</i> ×100%] [%]	–	↓ −0.88	↓ −6.55	↑ 4.72	↓ −1.61	↓ −0.58	↓ −6.36
<i>NvM</i> [MPa]	294.60	277.20	248.85	244.71	260.65	266.02	249.16
<i>NvM</i> value relative to <i>MB1</i> [(<i>NvMA</i> − <i>NvMB</i>)/ <i>NvMB</i> ×100%] [%]	–	↓ −5.91	↓ −15.53	↓ −16.94	↓ −11.52	↓ −9.70	↓ −15.42
<i>O</i> [mm ³]	159460.64	100434.58	108379.75	104186.59	118110.96	129297.44	106070.68
<i>O</i> value relative to <i>MB1</i> [(<i>OA</i> − <i>OB</i>)/ <i>OB</i> ×100%] [%]	–	↓ −37.02	↓ −32.03	↓ −34.66	↓ −25.93	↓ −18.92	↓ −33.48
<i>I3</i> [kg/mm ²]	1229.04	913.44	951.01	928.71	995.66	1093.00	941.72
<i>I3</i> value relative to <i>MB1</i> [(<i>I3A</i> − <i>I3B</i>)/ <i>I3B</i> ×100%] [%]	–	↓ −25.68	↓ −22.62	↓ −24.44	↓ −18.99	↓ −11.07	↓ −23.38

Note: 1) *P* – displacement (max); 2) *PA* – the value of the displacement (max) of the analysed gear; 3) *PB* – the value of the displacement (max) of the *MB1* gear; 4) *PZ* – displacement along *Z*-axis (max); 5) *PZA* – the value of the displacement along *Z*-axis (max) of the analysed gear; 6) *PZB* – the value of the displacement along *Z*-axis (max) of the *MB1* gear; 7) *NvM* – von Mises stress (max) [MPa]; 8) *NvMA* – the value of the von Mises stress (max) of the analysed gear; 9) *NvMB* – the value of the von Mises stress (max) of the *MB1* gear; 10) *O* – volume; 11) *OA* – the value of the volume of the analysed gear; 12) *OB* – the value of the volume of the *MB1* gear; 13) *I3* – principal moment of inertia; 14) *I3A* – the value of the principal moment of inertia of the analysed gear; 15) *I3B* – the value of the principal moment of inertia of the *MB1* gear

disc gear, *MB4* shell gear, and *MB6* gear with bean-shaped holes are the highest and reach a value about 35% higher than the gear which is the reference for the analysis performed – *MB1*. However, for the *MB3* ribbed disc gear and the *MB5* honeycomb gear, the parameter under consideration takes on a value higher by 19÷25% in relation to the *MB1* solid gear. The *MB7* ribbed disc gear with holes takes on a value about 30% higher than the *MB1* solid gear.

The value of displacement along the *Z*-axis (max) [mm] for the gear *MB2* with the disc and for the gear *MB6* with bean-shaped holes is the smallest (relative to the *MB1* base gear it is about 1% smaller) (Fig. 7, Fig. 12). However, for the

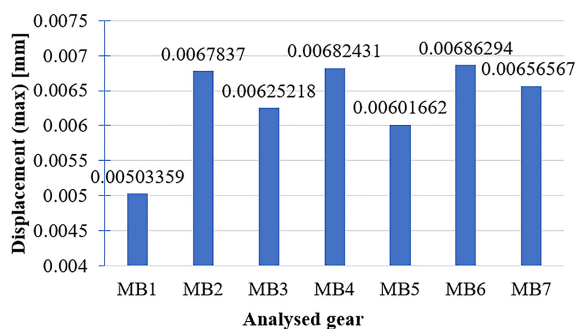


Fig. 7. Obtained values of the displacement (max) [mm]

MB3 ribbed disc gear, *MB4* shell gear, and *MB7* ribbed disc gear with holes, it is greatest – it is within ±7% relative to the *MB1* solid gear without modification (Fig. 12).

The von Mises stress (max) value [MPa] relative to the *MB1* base gear for the *MB2* disc gear had the least reduction (Fig. 9) of about 6% (Fig. 12). For the *MB3* ribbed disc gear, *MB4* shell gear, and the *MB7* ribbed disc gear with holes, the maximum von Mises stress values are comparable (Fig. 9), and relative to the *MB1* base gear, they decreased by about 16% (Fig. 12).

The *MB2* disc, *MB3* ribbed disc, *MB4* shell, and *MB7* ribbed disc with holes gears experienced the greatest volume reduction and thus

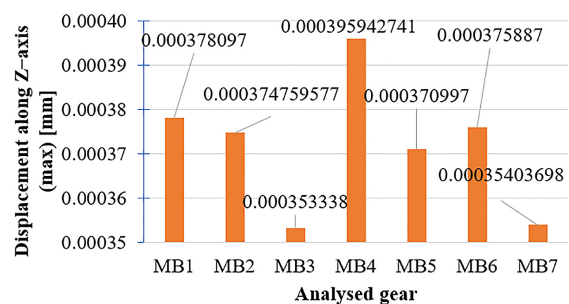


Fig. 8. Obtained results of the displacement along *Z*-axis (max) [mm]

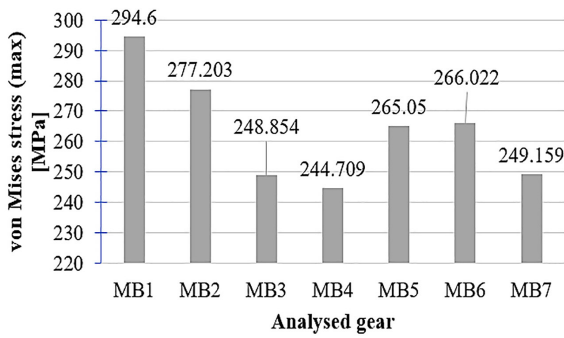


Fig. 9. Values of the von Mises stress (max) [MPa]

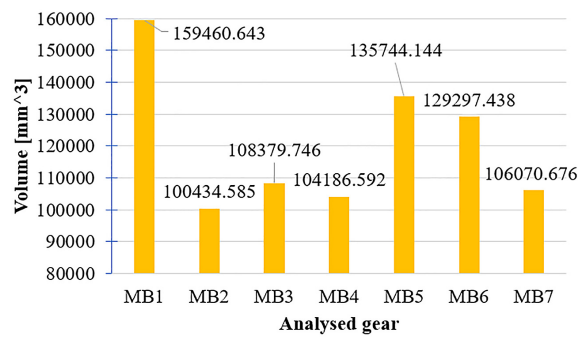


Fig. 10. Comparison of the Volumes [mm³] of the analysed weight-reduced gears

weight reduction (Fig. 10) of over 32% relative to the unmodified *MB1* gear (Fig. 12).

The 10 mm thick disc *MB2*, 10 mm thick ribbed disc *MB3*, shell *MB4*, and ribbed disc with holes *MB7* gears achieved similar values of

Principal moment of inertia *I3* [kg/mm²] (Fig. 11) and declined from the base gear *MB1* by more than 20% (Fig. 12). The *MB5* honeycomb gear and the *MB6* bean-shaped holes gear had the

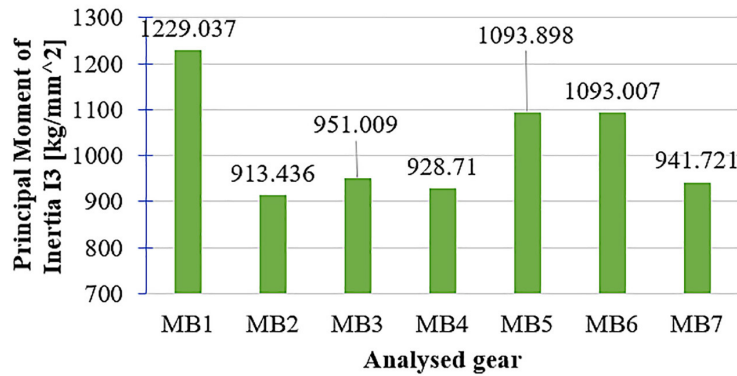


Fig. 11. Obtained values of the Principal Moment of Inertia *I3* [kg/mm²]

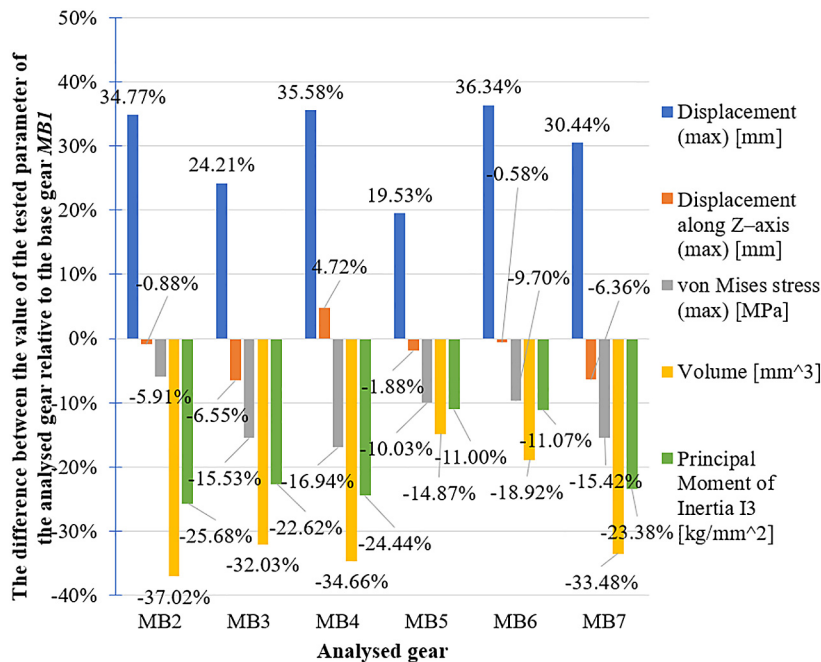


Fig. 12. Summary of the analysed parameters in relation to the *MB1* solid gear

smallest decrease in principal moment of inertia relative to the *MB1* base gear by 11% (Fig. 12).

It can be seen from Figure 12 that the obtained values of the analysed parameters of the *MB2* disc, *MB3* ribbed disc, *MB4* shell, and *MB7* ribbed disc with holes gears are close to each other and reach similar values with respect to the *MB1* base gear.

Figures 13 and 14 show the obtained displacement and von Mises stress distributions for the analysed structural solutions.

CONCLUSIONS

Reducing the weight of the gear transmission is of particular importance in the aviation and automotive industries due to, among others, the reduction of the negative impact of dynamic phenomena occurring during the operation of the gear transmission. First of all, gears with reduced mass, made by injection methods from polymer materials, are used in household appliances, in which, thanks to their use, one can notice, among

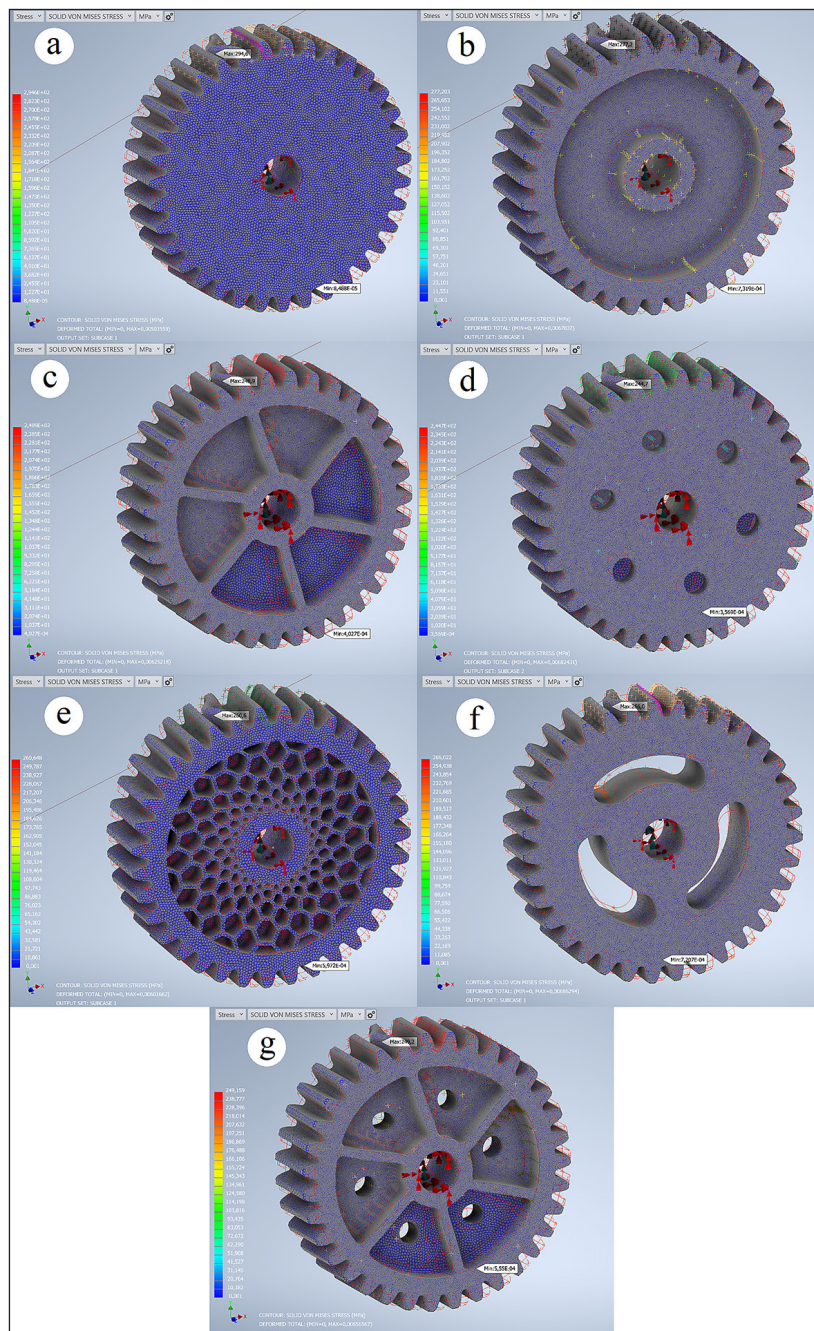


Fig. 13. Von Mises stress (max) [MPa] distribution for *MB1* (a), *MB2* (b), *MB3* (c), *MB4* (d), *MB5* (e), *MB6* (f) and *MB7* (g)

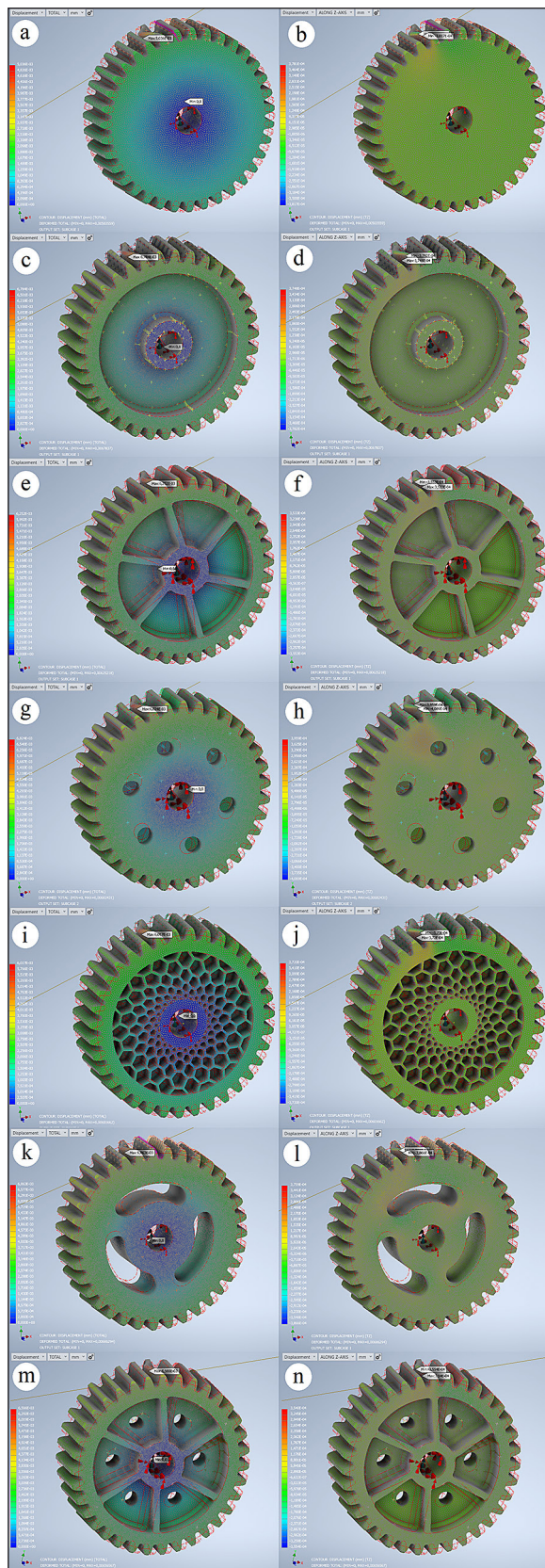


Fig. 14. Displacement (max) [mm] and displacement along Z-axis (max) [mm] distributions for: *MB1* (a, b), *MB2* (c, d), *MB3* (e, f), *MB4* (g, h), *MB5* (i, j), *MB6* (k, l) and *MB7* (m, n)

others, reducing material consumption, reducing the mass of the entire system, reducing dynamic surpluses, and damping vibrations. Such gears also allow for lubrication-free operation and are often used with metal gears whereby the sound intensity that occurs with the interaction of the metal gears is reduced.

Knowledge of the strength properties of weight-reduced gears enables their proper design to guarantee the transfer of a given load under specified initial conditions. Also, static analysis in the MES environment will allow the determination of deformations and strains that can have a significant impact on the strength of the analysed gear, and which can be eliminated to some extent, or their impact can be minimized already at the design stage before their final production.

The research presented in this paper was aimed at the analysis of selected design solutions of weight-reduced gears with a changed disc geometry, keeping in mind a relatively constant stress level while reducing the weight as much as possible. It is worth mentioning that while designing the construction of the disc as well as the gear wheel itself, you should take into account the manufacturing process that will be used to produce the considered gears, the material from which the elements are to be made and the working conditions they are to meet. Based on the analysis of selected design solutions of gears with reduced weight, it was found that there is no linear relation between the reduction in weight and the reduction in the considered strength parameters. Considering the analysis performed, it can be noticed that the most favourable solution is the gear with a 10 mm thick *MB3* ribbed disc due to the similar values of displacements obtained in relation to the *MB1* solid gear (increase in displacement (max) by over 24% and decrease in displacement along the Z axis (max) by over 6% in relation to the *MB1* base gear (Fig. 12)), as well as a significant reduction of the principal moment of inertia (by about 32% in relation to the *MB1* solid gear (Fig. 12)) and decrease in weight, and thus volume (decrease by over 32% in relation to the *MB1* base gear (Fig. 12)). The greatest reductions in weight, and thus volume, relative to the *MB1* solid gear except for the *MB3* gear (with a ribbed disc) were the *MB2* gear with a 10 mm thick disc at the center (down more than 37%), the *MB4* shell gear (down more than 34%) and the *MB7* ribbed disc gear with holes (down more than 33%) (Fig. 12). The *MB3* and

MB7 gears are gears of similar geometry, but the *MB7* gear also has cylindrical holes. Comparing the results of the analysed parameters for both gears, it can be concluded that the values of the displacement along the *Z*-axis (max), von Mises stress (max), volume and the principal moment of inertia are similar – only the *MB7* gear achieves higher values of displacement (max) than *MB3* gear (Fig. 12). In addition, further work should be undertaken to investigate the *MB5* honeycomb gear, as this gear achieved the lowest difference in displacement (max) values (a decrease of about 20% relative to the *MB1* solid gear (Fig. 12)) and one of the lower differences in displacement along the *Z*-axis (max) (a decrease of about 2% relative to the *MB1* base gear (Fig. 12)) and von Mises stress (max) (a decrease of more than 10% relative to the *MB1* solid gear (Fig. 12)) relative to the *MB1* base gear among the gears analysed.

REFERENCES

- Sobolewski B., Budzik G. and Dziubek T. Analiza rozwiązań konstrukcyjnych kół zębatych o zmniejszonej masie. *Autobusy*. 2017; 10/2017: 37–39.
- Singh P.K. and Saini R. Static analysis of epoxy resin and carbon fibre composite spur gear. *Materials Today: Proceedings*. 2022; 50(5): 2443–2449. <https://doi.org/10.1016/j.matpr.2021.10.289>
- Khanna R. and Sinha P.K. Structural Analysis of Spur Gear with Composite Material Under Different Loading Conditions. in *Recent Advances in Mechanical Engineering*. Singapore: Springer. 2021; 599–604.
- Singh P.K., Mausam K. and Islam A. Achieving better results for increasing strength and life time of gears in industries using various composite materials. *Materials Today: Proceedings*. 2021; 45(2):3068–3074. <https://doi.org/10.1016/j.matpr.2020.12.062>
- Wojnar G. and Juzek M. The impact of non-parallelism of toothed gear shafts axes and method of gear fixing on gearbox components vibrations. *Acta Mechanica Et Automatica*. 2018; 12(2): 165–171. DOI: 10.2478/ama-2018–0026
- Rajeshkumar S. and Manoharan R. Design and analysis of composite spur gears using finite element method. *IOP Conference Series: Materials Science and Engineering*. 2017; 263(6). <https://doi.org/10.1088/1757-899X/263/6/062048>
- Chawathe D.D. *Handbook of Gear Technology*. New Age International Publication. 2011; 26–89, 305–536, 579–706.
- Muminovic A.J., Colic M., Mesic E. and Saric I. Innovative design of spur gear tooth with infill structure. *Bulletin of the Polish Academy of Sciences: Technical Sciences*. 2020; 68(3). DOI: 10.24425/bpasts.2020.133370
- Chavadaki S., Nithin Kumar K.C. and Rajesh M.N. Finite element analysis of spur gear to find out the optimum root radius. *Materials Today: Proceedings*. 2021; 46(20): 10672–10675. <https://doi.org/10.1016/j.matpr.2021.01.422>
- Karuppanan S. and Patil S. Frictional stress analysis of spur gear with misalignments. *Journal of Mechanical Engineering and Sciences*. 2018; 12(2): 3566–3580. <https://doi.org/10.15282/jmes.12.2.2018.4.0316>
- Vunnam Naga Sai, Kakumani Venkata Siva Prasad, Jangala Sai Sri Laxman and P.S. Rama Sreekanth. Comparative analysis and simulation of metal and non-polymer composite gears. *Materials Today: Proceedings*, Nov. 2021. [Online]. Available: <https://doi.org/10.1016/j.matpr.2021.10.174> [Accessed: 12 Nov. 2021]
- Lisle T.J., Shaw B.A. and Frazer R.C. Internal spur gear root bending stress: A comparison of ISO 6336:1996, ISO 6336:2006, VDI 2737:2005, AGMA, ANSYS finite element analysis and strain gauge techniques. *Proceedings of the Institution of Mechanical Engineers, Part C: Journal of Mechanical Engineering Science*. 2019; 233(5): 1713–1720. <https://doi.org/10.1177/2F0954406218774364>.
- Shaik M.A.R., Kumar E.P. and Basha S.S. Finite Element Analysis and Fatigue Analysis of Spurgear under Random Loading. *International Journal of Scientific Engineering and Technology Research*. 2017; 6(30): 5854–5858.
- Tchórz T., Śniezek L. and Grzelak K. Contact Fatigue Strength of 21NiCrMo2 Steel Gears Subjected to Shot Peening Treatment. *AIP Conference Proceedings: Fatigue Failure and Fracture Mechanics XXVII*. 2018; 2028. <https://doi.org/10.1063/1.5066411>
- Wang Z.G., Hirasawa K., Yoshikawa Y. and Osaka K. Forming of light-weight gear wheel by plate forging. *CIRP Annals-Manufacturing Technology*. 2016; 65(1): 293–296. <https://dx.doi.org/10.1016/j.cirp.2016.04.134>
- Tekkaya A.E., Khalifa N.B., Grzancic G. and Hölker R. Forming of Lightweight Metal Components: Need for New Technologies. *Procedia Engineering*. 2014; 81: 28–37. <https://doi.org/10.1016/j.proeng.2014.09.125>
- Varun S.R., Govindaraju M., Ramu M. and Satheshkumar V. Influence of Metal Foam Properties on Performance of Polymer Composite Materials. *Materials Today: Proceedings*. 2020; 24(2): 1244–1250. <https://doi.org/10.1016/j.matpr.2020.04.439>

18. Muminovic A.J., Muminovic A., Mesic E., Saric I. and Pervan N. Spur Gear Tooth Topology Optimization: Finding Optimal Shell Thickness for Spur Gear Tooth produced using Additive Manufacturing. *TEM Journal*. 2019; 8(3): 788–794. DOI: 10.18421/TEM83–13
19. Höhn B.-R., Michaelis K. and Wimmer A. Low loss gears. *Gear Technology*. 2007; 28–35.
20. Magalhães L., Martins R., Locateli C. and Seabra J. Influence of tooth profile and oil formulation on gear power loss. *Tribology International*. 2010; 43(10): 1861–1871. <https://doi.org/10.1016/j.triboint.2009.10.001>
21. Höhn B.-R., Michaelis K. and Doleschel A. Frictional behaviour of synthetic gear lubricants. *Tribology Series*. 2001; 39: 759–768. [https://doi.org/10.1016/S0167-8922\(01\)80156-5](https://doi.org/10.1016/S0167-8922(01)80156-5)
22. Major B., Sandu A.V., Abdullah M.M.A.B., Nabiałek M., Tański T. and Zieliński A. Modern materials- obtaining and characterization (alloys, polymers). *Bulletin of the Polish Academy of Science: Technical Science*. 2021; 69(5). DOI: 10.24425/bpasts.2021.139318
23. Mao K., Langlois P., Madhav N., Greenwood D. and Millson M. A Comparative study of Polymer Gears Made of Five Materials. *Gear Technology*. 2019; 68–72.
24. Singh A.K. and Singh P.K. Polymer spur gears behaviours under different loading conditions: A review. *Proceedings of the Institution of Mechanical Engineers, Part J: Journal of Engineering Tribology*. 2018; 232(2): 210–228. DOI: 10.1177/1350650117711595
25. Ondrušová D., Labaj I., Pajtášová M., Vršková J., Božeková S., Feriancová A. and Skalková P. Target modification of the composition of polymer systems for industrial applications. *Bulletin of the Polish Academy of Sciences: Technical Sciences*. 2021; 69(2). DOI: 10.24425/bpasts.2021.136721
26. Zhenglong Z., Bin S., Jiangang L., Zhiguang D. and Zhongbo H. Research on ride comfort performance of a metal tire. *Bulletin of the Polish Academy of Sciences: Technical Sciences*. 2020; 68(3): 491–502. DOI: 10.24425/bpasts.2020.133384
27. Oleksy M. *Materiały polimerowe stosowane na elementy maszyn*. Rzeszów: Oficyna Wydawnicza Politechniki Rzeszowskiej, 2019; 113–116.
28. *Konstrukcje z tworzyw sztucznych. Praktyczny poradnik zasady doboru materiałów*. Warszawa: Wydawnictwo Informatyzacji Zawodowej ALFA-WEKA Sp. z o. o., 1997.
29. Markowski T., Budzik G., Kozik B., Dziubek T., Sobolewski B. Modeling 3D CAD and Rapid Prototyping the presenter planetary gear. *Scientific Journal of Silesian University of Technology– Series Transport*. 2014; 83: 155–162.
30. Przeszłowski Ł., Budzik G., Dziubek T. and Sobolewski B. Toothed wheel and method for manufacturing of the toothed wheel. *Poland Patent Pat.236610*, Apr. 2018.